Electronic structure and interatomic bonding in $Al_{10}V$

2003 J. Phys.: Condens. Matter 15 5675

(http://iopscience.iop.org/0953-8984/15/33/302)

INSTITUTE OF PHYSICS PUBLISHING JOURNAL OF PHYSICS: CONDENSED MATTER

J. Phys.: Condens. Matter **15** (2003) 5675–5688 PII: S0953-8984(03)65535-9

Electronic structure and interatomic bonding in $Al_{10}V$

M Jahnátek[1,2], M Krajčí[1,2] and J Hafner[2]

[1] Institute of Physics, Slovak Academy of Sciences, Dúbravská cesta 9, SK 84228 Bratislava, Slovakia
[2] Institut für Materialphysik and Centre for Computational Materials Science, Universität Wien, Sensengasse 8/12, A-1090 Wien, Austria

E-mail: fyzikraj@savba.sk

Received 1 July 2003
Published 8 August 2003
Online at stacks.iop.org/JPhysCM/15/5675

Abstract

On the basis of *ab initio* calculations we analysed the electron density distribution in the elementary cell of the compound $Al_{10}V$. We found covalent bonding between certain atoms. The Al–V bonds of enhanced covalency are linked into $\cdots$–Al–V–Al–V–$\cdots$ chains that extend over the whole crystal. The chains intersect at each V site and together form a Kagomé network of corner-sharing tetrahedra. The large voids of this network are filled by Z_{16} Friauf polyhedra consisting of Al atoms only. The skeleton of the Friauf polyhedron has the form of a truncated tetrahedron and consists of 12 strongly bonded Al atoms. These Al–Al bonds also have covalent character. The bonding is dominated by sp^2 hybridization. The centre of the Friauf polyhedron may be empty or occupied by an Al atom. The thermodynamic stability of the phase is investigated. The $Al_{21}V_2$ phase with occupied voids is at low temperatures less stable than $Al_{10}V$. The $Al_{10}V$ structure can be considered as a special case of the $Al_{18}Cr_2Mg_3$ structural class. We have found the same picture of bonding as we report here for $Al_{10}V$ for several other aluminium-rich alloys belonging to the $Al_{18}Cr_2Mg_3$ structural class also.

1. Introduction

Transition metal (TM) aluminides are known to be of great technological importance and high scientific interest. Al-based nanocrystalline compounds of TMs are among the most promising candidate high-performance structural materials [1]. The reported tensile strength of e.g. nanocrystalline $Al_{94}V_4Fe_2$ is above 1300 MPa, which exceeds the strength of usual technical steels [2]. The physical interest in TM aluminides is triggered by the wide variety of physical properties: aluminides form an important class of quasicrystals, with exotic physical and chemical properties [3]. TM aluminides may also exhibit true semiconducting behaviour [4, 5]. In this paper we continue our investigation of physical properties of aluminium-rich vanadium compounds. Very recently, we have performed a

Table 1. Crystallographic data for the $Al_{10}V$ structure. The lattice constant is 14.492 (14.460) Å. Values in brackets are results obtained from the *ab initio* calculations. The elementary cell consists of 176 atoms. 'Type E' marks positions of the voids in the structure. The voids can be occupied by Al atoms. CN is the coordination of the site and V_V is volume of the corresponding Voronoi cell.

Type	Wyckoff	x	y	z	CN	V_V
V	16c	0.1250	0.1250	0.1250	12	11.78
Al_1	16d	0.6250	0.6250	0.6250	14	19.85
Al_2	48f	0.1407	0.0000	0.0000	12	15.56
		(0.1404)	0.0000	0.0000		
Al_3	96g	0.0654	0.0654	0.3009	12	16.94
		(0.0650)	(0.0650)	(0.3026)		
E	8b	0.5000	0.5000	0.5000	16	20.52

detailed study for Al_3V [6]. NMR studies suggest a strong directional bonding in Al_3V [7, 8]. This conjecture is further corroborated by the structural analysis: the unusually short Al–V distances [9] indicate that the bonding may have a covalent character. Our investigation of the interatomic bonding in this compound has confirmed and extended these conjectures.

Physical properties and interatomic bonding in $Al_{10}V$ seem to be even more extraordinary and deserve a detailed investigation. Caplin *et al* [9] performed low-temperature specific heat and electrical resistivity measurements on the $Al_{10}V$ compound. They showed that this compound has a local soft mode with a characteristic temperature of 22 K. Its behaviour is well described by an Einstein model. The number of such modes, together with x-ray evidence, indicates that the mode is associated with a loose Al atom occupying a large hole in the $Al_{10}V$ structure. This and other peculiarities of the structure provide evidence for strong and unusual bonding effects [9].

The structure of $Al_{10}V$ is rather peculiar. It may be seen as a 'superstructure' of the C15 Laves phase Cu_2Mg type in which the Mg and Cu atoms are replaced by larger many-atom complexes. The role of the big Mg atom is assumed by a Friauf polyhedron [10] consisting of Al atoms. In the C15 structure, the smaller Cu atoms form a three-dimensional polytetrahedral Kagomé network in which the larger atoms are embedded. In $Al_{10}V$ the V atoms occupy the vertices of the Kagomé network, with Al atoms occupying the mid-bond sites. The structure is thus a packing of the Friauf polyhedra in a diamond lattice reinforced by strongly bonded chains of alternating vanadium and aluminium atoms forming a tetrahedral network that extends over the whole crystal. $Al_{10}V$ is a stable low-temperature phase [11]. This phase precipitates at crystallization of an amorphous matrix in the high-strength $Al_{94}V_4Fe_2$ alloy. Although the enhanced strength of this alloy has its origin primarily in its nanoscale structure, knowledge of the interatomic bonding can also be very helpful for understanding the unusual mechanical properties of these alloys.

2. Crystal structure

$Al_{10}V$ is an intermetallic compound with the cF176 crystal structure [12]. Its space group is $Fd\bar{3}m$ (No 227). The primitive cell contains 44 atoms. The cubic elementary cell consists of four primitive cells. The crystallographic data are listed in table 1. The structure has relatively very high symmetry. All 176 atomic sites of the unit cell are generated by symmetry operations from only four crystallographic sites. There are only three internal degrees of freedom. In table 1, in addition to the crystallographic data we present also optimized coordinates from a relaxation of the structure by Hellmann–Feynman forces. The agreement of the calculated quantities with experimental ones is excellent; see section 3.

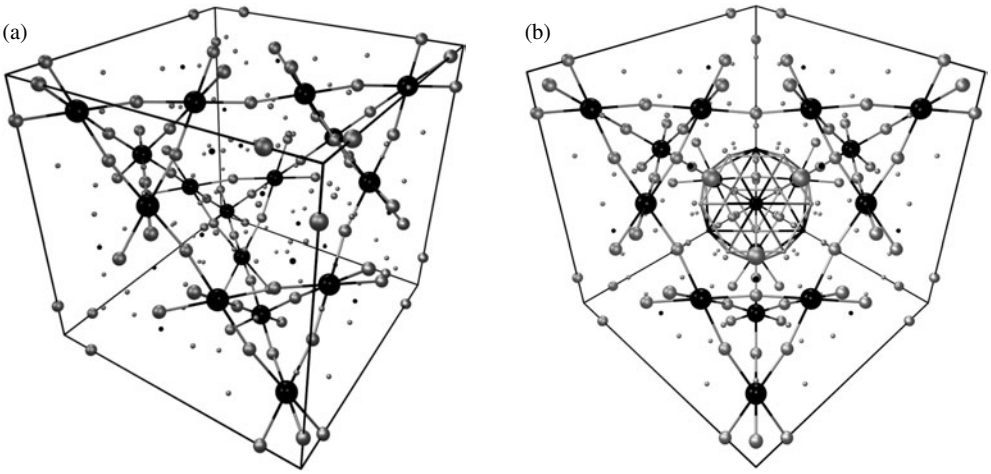

Figure 1. An elementary cell of $Al_{10}V$. Positions of aluminium atoms are represented by small spheres; positions of vanadium atoms are represented by big dark spheres. (a) Vanadium atoms bonded to Al_2 atoms form a tetrahedral network consisting of large and small tetrahedra. (b) The view along the body diagonal of the Friauf polyhedron that exists inside each large tetrahedron. There are eight such Friauf polyhedra per unit cell located at the sites of a diamond lattice. Each Friauf polyhedron is vertex-connected with four neighbouring Friauf polyhedra via the Al_1 atoms represented by small dark spheres.

A peculiar feature of the structure is the existence of relatively large voids in the elementary cell. There are two such voids per primitive cell. The voids can be empty or occupied by Al atoms. It is remarkable that the size of the void is larger than the diameter of the Al atom. While the characteristic diameter of an Al atom is 2.8 Å, the diameter of the void is ≈3.2 Å. The composition of the sample can vary from $Al_{90.9}V_{9.1}$ to $Al_{91.3}V_{8.7}$. The limiting compositions $Al_{10}V$ and $Al_{21}V_2$ correspond to the structures with voids that are empty and fully occupied by Al atoms, respectively.

In the elementary cell there are three aluminium sites (Al_1(16d), Al_2(48f), and Al_3(96g)) and one vanadium crystallographic site V (Wyckoff notation 16c). The void (8b) is surrounded by a polyhedron of Al atoms. The polyhedron has a regular shape and can be identified as a Z_{16} Friauf polyhedron; see figures 1 and 2. It consists of four Al_1 and 12 Al_3 atoms. The polyhedron has thus 16 vertices, 28 regular triangular faces, and 42 edges. The edges around Al_1 have sixfold symmetries and the edges around the Al_3 atoms have fivefold symmetries. Two neighbouring polyhedra share one vertex site occupied by the Al_1 atom.

Each vanadium atom has six Al_2 neighbours and six Al_3 neighbours forming together a distorted icosahedron. The distance between V and Al_3 neighbours is $d(\text{V–Al}_3) = 2.826$ Å. The distance between V and Al_2 neighbours is unusually short: $d(\text{V–Al}_2) = 2.572$ Å. This indicates strong V–Al_2 bonding. Vanadium and Al_2 atoms form linear chains consisting of alternating V and Al atoms. The chains extend through the whole crystal. In each vanadium atom three such chains intersect. The chains form large and small tetrahedra, as displayed in figure 1(a). Inside each large tetrahedron there is one Friauf polyhedron; see figure 1(b). Large tetrahedra formed of strongly bonded V–Al_2 chains thus reinforce the Friauf polyhedra from outside.

As already noted above, the $Al_{10}V$ structure may also be seen as a superstructure of the C15 Laves phase Cu_2Mg type. In Cu_2Mg, big Mg atoms occupy the positions of a diamond lattice. Smaller Cu atoms form a tetrahedral network consisting of a set of intersecting planes

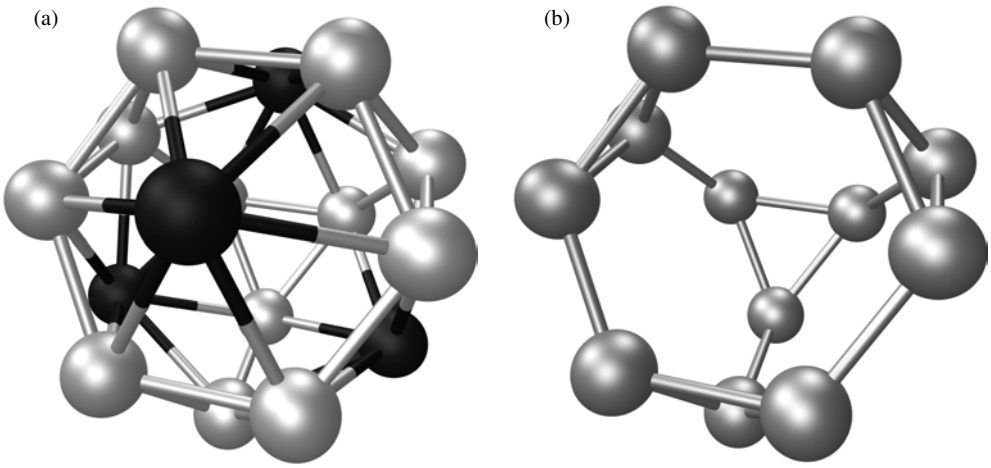

Figure 2. (a) The Friauf polyhedron consists of 16 aluminium atoms. Four Al_1 atoms represented by darker spheres are at vertices of a tetrahedron. The other twelve Al_3 atoms are represented by lighter spheres; they occupy the vertices of a truncated larger tetrahedra. The centre of the Friauf polyhedron may be empty or occupied by an Al atom. (b) The skeleton of the Friauf polyhedron consisting of Al_3 atoms is a strongly bonded structure. Between pairs of neighbouring Al_3 atoms, bonds with enhanced covalency were found.

oriented in tetrahedral directions. Each plane has the form of a Kagomé network. In the $Al_{10}V$ structure the role of the big Mg atom is played by the Friauf polyhedron and the Kagomé network is formed by chains of alternating V and Al atoms.

The analysis of the coordination polyhedra sheds further light on the correlation between the C15 and $Al_{10}V$ structures. In the Laves phase the larger minority atoms (Mg) at the 8b Wyckoff sites are coordinated also by a Friauf polyhedron, with the sixfold vertices occupied by other Mg atoms and the fivefold vertices by smaller Cu atoms. In $Al_{10}V$ the vertices of a large Friauf polyhedron are occupied by twelve V atoms and four Al–Friauf clusters. The small Al–Friauf polyhedron and the large 'super-Friauf' polyhedron are concentric and have the same orientation, such that there are straight Al_3–V–Al_3 bonds linking the Al clusters and the Al–V Kagomé network.

A similar relation exists between the distorted icosahedron of Al_2 and Al_3 atoms surrounding V and a larger concentric icosahedron whose vertices are occupied by six V atoms and six Al–Friauf clusters. The linking between these icosahedra is provided both by the Al_2–V bonds in the Kagomé network and the Al_3–V–Al_3 bonds discussed above.

The $Al_{10}V$ structure is a special case of a wider structural class, $Al_{18}Cr_2Mg_3$ [13]. In this structural class there exist the same Friauf polyhedra but here their centres are not empty but occupied by Mg atoms. Other Mg atoms are at sites of the Al_1 atoms. The Voronoi analysis of the $Al_{10}V$ structure—see table 1—reveals that the volume of the Voronoi cell at Al_1 at the 16d site is 19.85 Å^3, which is a value only a little smaller than 20.52 Å^3, the volume of the Voronoi cell of the void in the centre of the Friauf polyhedron at the 8b site. The Al_1 atoms in the $Al_{10}V$ structure can thus be easily replaced by bigger Mg atoms in the $Al_{18}Cr_2Mg_3$ structure.

In the following sections we shall investigate the electronic structure of this peculiar system in order to obtain an understanding of the stability of this relatively open structure. We studied the interatomic bonding by investigating the charge density distribution and by calculating the crystal orbital overlap population (COOP) defined by Hoffmann [14] for selected configurations of atoms. Covalent bonds between the V and Al atoms were identified

from an enhanced charge density along the connections between the atoms. The COOP calculated for configurations of symmetrized orbitals revealed a bonding–antibonding splitting of the orbitals, thus confirming the covalent character of the bonds.

3. Methodology

The electronic structure calculations were performed using two different techniques. The plane-wave-based Vienna *ab initio* simulation package VASP [15, 16] was used for the calculations of the electronic ground state and for the optimization of the atomic volume and unit-cell geometry of $Al_{10}V$. The VASP program was also used to calculate charge distributions. In its projector-augmented-wave (PAW) version [16], VASP calculates the exact all-electron eigenstates; hence it can produce realistic electron densities. The plane-wave basis allows one to calculate Hellmann–Feynman forces acting on the atoms and stresses on the unit cell. The total energy may by optimized with respect to the volume and the shape of the unit cell and to the positions of the atoms within the cell.

However, a plane-wave-based approach such as that used in VASP produces only the Bloch states and the total density of states (DOS), a decomposition into local orbitals and local orbital-projected DOSs requiring additional assumptions. To achieve this decomposition, self-consistent electronic structure calculations have been performed using the tight-binding linear muffin-tin orbital (TB-LMTO) method [17–19] in an atomic-sphere approximation (ASA) using the optimized structure produced by VASP. The minimal LMTO basis includes s, p, and d orbitals for each Al and V atom. The two-centre TB-LMTO Hamiltonian has been constructed and diagonalized using the standard diagonalization techniques. The total DOS and the band structures produced by both VASP and TB-LMTO techniques are found to be in good agreement. The TB-LMTO basis is used to construct the symmetrized hybrid orbitals from which the COOPs are calculated.

3.1. Calculated crystal structure

The optimized crystal structure parameters are summarized in table 1. The cubic lattice constant agrees with experiment within 0.25%. Within the unit cell only the x-parameter of the Al_2 sites and the x- and z-parameters of the Al_3 sites are not fixed by symmetry. The optimized parameters show excellent agreement with experiment, with deviation ranging between 0.003 and 0.0017. This corresponds to interatomic distances which agree with experiment typically within 0.02 Å. For the V–Al_2 distances along the chains discussed above, the accuracy is even higher. The calculated lattice constant is 14.46 Å; this is only 0.2% smaller than the experimental value. The volume per atom is expanded by 5.8% compared to the linear average of those of Al and V; see table 2. Such a volume expansion in an intermetallic compound is rather unusual, and is indicative of a substantial degree of covalency in the chemical bonding.

4. Electronic structure

The electronic structure of aluminium-rich Al–TM compounds typically exhibits a narrow TM d band superposed on a parabolic-like Al band. The total DOS is more or less modulated by van Hove singularities, bonding–antibonding d-band splitting, and possible hybridization effects. For transition metals the Fermi level is located in a region of high DOS, which results in characteristic metallic properties of the system. The electronic structure of $Al_{10}V$ has already been calculated by other authors [20]. As regards the form of the DOS, our results confirm the previous calculations. The DOS of $Al_{10}V$ is essentially a free-electron-like parabola strongly

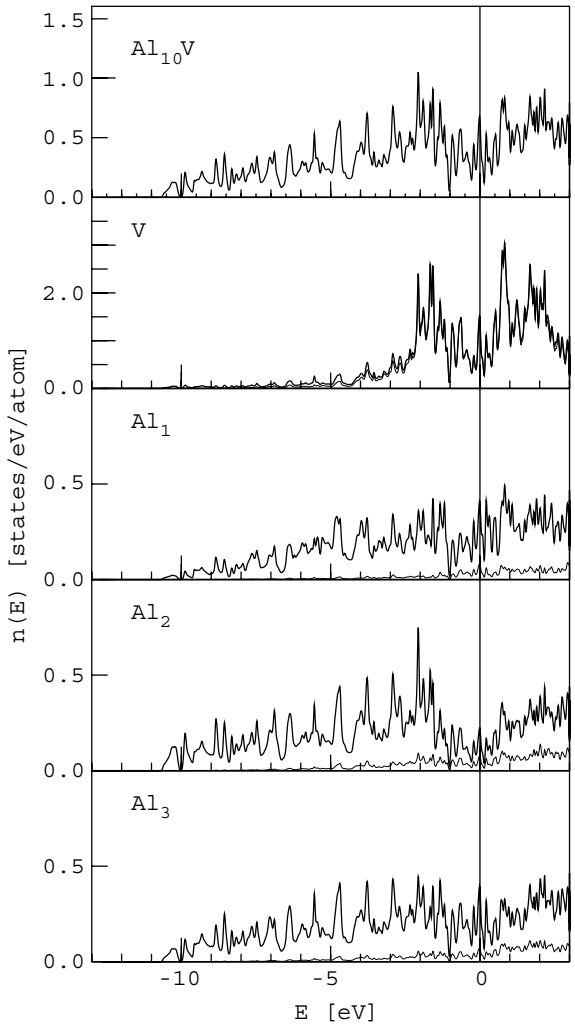

Figure 3. The DOS of $Al_{10}V$. From the top: the total DOS, the partial DOS on the vanadium atom, and partial DOSs on Al_1, Al_2, and Al_3 atoms. The thin line represents the contribution from d states.

modulated by van Hove singularities; see figure 3. Around the Fermi level one observes a mild depression extending from -2 to 2 eV. From the partial DOSs one can observe that this depression has its origin in the V and Al_2 contributions. Partial DOSs of both types of atom exhibit bonding–antibonding splitting that indicates strong interaction between V and Al_2 atoms.

5. Charge densities and bonding

Using the VASP program we calculated the charge density distribution in the elementary cell of the $Al_{10}V$ structure. Figure 4(a) shows a contour plot of the valence charge distribution in the (x, y) plane for $z = 0.125$. One can see a chain of alternating Al_2 and V atoms oriented along a diagonal direction in the figure. Such chains of atoms form the tetrahedral network

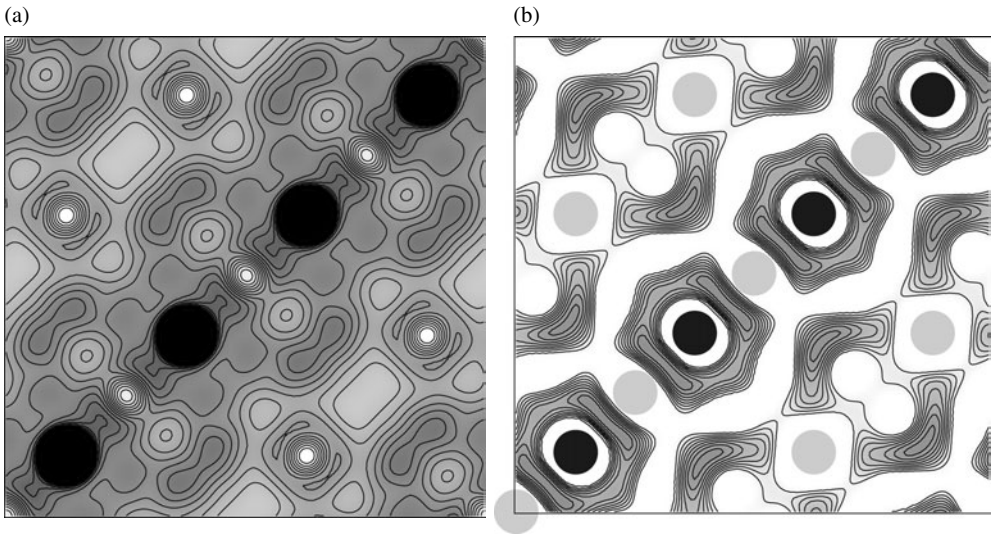

Figure 4. (a) A contour plot of the valence electron density in the (x, y) plane intersecting the $Al_{10}V$ elementary cell at $z = 0.125$. The high charge density in the centre—dark circles—corresponds to vanadium atoms. Positions of aluminium atoms are characterized by minima of charge density—light spots. Alternating vanadium and Al_2 atoms located along the diagonal form chains of bonded atoms; cf figure 1(a). Four aluminium atoms above and below the diagonal are Al_1 atoms. (b) A contour plot of the difference electron density in the same plane as in the previous figure. In the difference density a non-self-consistent charge density obtained as a superposition of atomic charge densities is subtracted from the total charge density. In the figure we represent only regions of enhanced density. In blank regions between atoms the difference density is negative. One can clearly identify enhanced charge density corresponding to bonding between the V atom and Al_2 atoms. Positions of vanadium and aluminium atoms are here represented by black and grey circles, respectively.

discussed in section 2; see also figure 1(a). The high charge densities (dark spots) correspond to the vanadium atoms. Positions of aluminium atoms are seen in the figure as light spots with minimal valence charge densities. If the character of the bonding is purely metallic, the charge distribution among atoms should be homogeneous. A possible covalent bonding is indicated by enhanced charge distributions along connections between atoms.

In figure 4(a) we see regions of enhanced charge density extending from a vanadium atom to both neighbouring Al_2 atoms. To see the covalent bonding more clearly we present also the difference electron density; i.e. a superposition of atomic charge densities is subtracted from the total charge density. The contour plot in figure 4(b) represents the regions of positive difference electron density in the (x, y) plane; in the blank space the difference density is negative. In this figure one can clearly identify the 'bond charges' between the V and Al_2 atoms.

A three-dimensional picture of the V–Al_2 bonding is seen in figure 1(a). At each vanadium atom three chains of bonds intersect. Each V atom is thus covalently bonded with six Al_2 atoms. These atoms together with the central V atom form an octahedron with a trigonal distortion. The length of the V–Al_2 bonds is 2.572 Å. We did not observe any substantial bonding between the V atom and the remaining six Al_3 neighbours located at a distance 2.826 Å from V near the plane perpendicular to the trigonal axes.

Another interesting interatomic bonding was found between the Al_3 atoms forming the skeleton of the Friauf polyhedron. Figure 5(a) shows the charge density at intersection of the

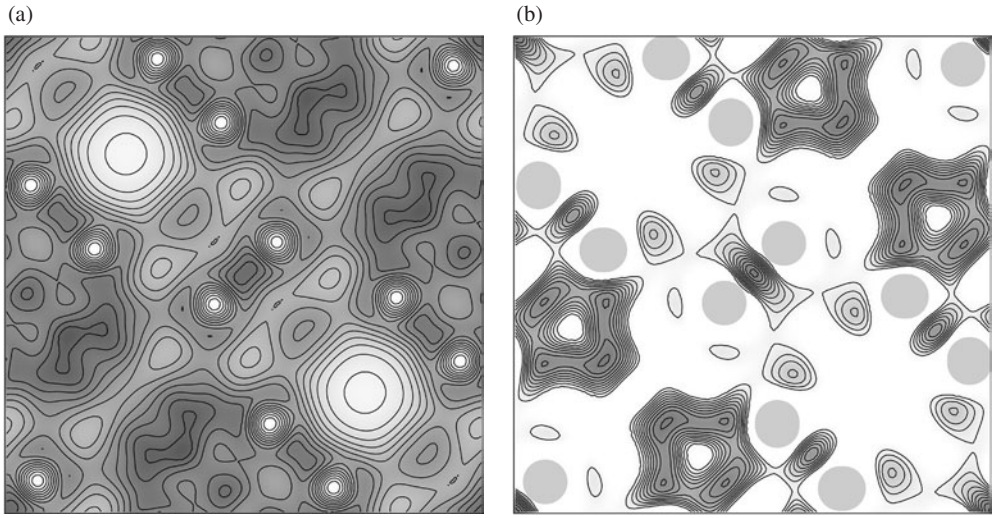

Figure 5. (a) A contour plot of the valence electron density in the (x, y) plane intersecting the $Al_{10}V$ elementary cell at $z = 0.301$. Two large regions of low charge density in the second and fourth quadrants of the figure are the empty centres of the Friauf polyhedra. All other light spots in the figure correspond to the positions of the Al_3 atoms. On the diagonal of the figure near the centre and near the upper-left and bottom-right corners, one can clearly see pairs of Al_3 atoms with significant bond charge between the atoms. Other pairs of Al_3 atoms surround the empty regions inside the Friauf polyhedra. (b) A contour plot of the difference electron density in the same plane as in the previous figure. One can clearly identify enhanced charge corresponding to bonding between pairs of Al_3 atoms. Positions of aluminium atoms are here represented by grey circles.

elementary cell in the plane $z = 0.3009$. The most striking features seen in the figure are two large regions of low charge density in the second and fourth quadrants of the figure. These regions correspond to the empty centres of the Friauf polyhedra. All other light spots in the figure correspond to the positions of the Al_3 atoms. On the diagonal of the figure near the centre and near the upper-left and bottom-right corners, one can clearly see pairs of Al_3 atoms with significant bond charge between the atoms. Other pairs of Al_3 atoms surround the empty regions inside the Friauf polyhedra. There it is also possible to recognize a significant bonding. The bonding is again more clearly seen in the difference electron density in figure 5(b). Al_3 atoms form the skeleton of the Friauf polyhedron. A three-dimensional picture of this skeleton appears in figure 2(b). The skeleton consists of twelve Al_3 atoms. It is remarkable that each Al_3 atom has just three nearest neighbours in this structure. This suggests sp^2 bonding between them and this conjecture will be proven in section 6. The skeleton of the Friauf polyhedron consists of four triangles of atoms; see figure 2(b). The bonds between the Al_3 atoms that are in figure 5 on the diagonal correspond to bonding between two triangles. The bonds between the off-diagonal pairs of Al_3 correspond to the bonding inside the triangle. The skeleton of the Friauf polyhedron has the shape of a truncated tetrahedron. To complete the Friauf polyhedron, one has to add four Al_1 atoms. It is interesting that the Al_1 are bonded to the rest of the Friauf polyhedron only very weakly. We did not find any enhanced charge density between Al_1 atoms and the neighbouring Al_3 atoms.

In summary, there are two types of covalent bond in the $Al_{10}V$ structure. Each vanadium atom has six bonds with Al_2 atoms. Each Al_3 atom is bonded with three other Al_3 atoms. The character of the bonds is investigated in the next section.

6. Hybridized orbitals and covalent bonding

To gain a deeper understanding of the bonds identified in the density contour plots, we attempted to construct sets of symmetrized hybridized orbitals oriented along the bonds, and calculated the DOS projected onto bonding and antibonding combinations of these symmetrized orbitals. The difference (B − A) between the bonding (B) and antibonding (A) projected densities is essentially equivalent to the differential COOP defined by Hoffman [14]. The symmetrized orbitals are sets of hybridized orbitals possessing the point group symmetry of a particular atomic site. A set of bonds originating from a particular atom forms a reducible representation of the point group. Decomposition of the reducible representation into irreducible ones enables one to select individual s, p, or d orbitals whose linear combinations form the hybridized orbitals.

6.1. Bonding between V and Al atoms in the tetrahedral network

From the charge density analysis we found that the characteristic configuration of bonding of a vanadium atom with the neighbouring Al_2 atoms has the form of an octahedron distorted along a trigonal axis. In another view of this bonding configuration it can be imagined as two inversely oriented trigonal pyramids joined at one vertex occupied by a vanadium atom.

From the vanadium side the bonding is mediated by s and d orbitals. The contribution of p states to the vanadium DOS is negligible, as is also seen in figure 3. As the orbital quantum number l for both s and d orbitals is even, the hybridized orbitals on the V atom will always have an inversion symmetry. The bonding of the six Al_2 atoms to V consists of three equivalent Al_2–V–Al_2 linear bonding configurations with the Al_2 atoms located in opposite directions from the central V atom. From the side of Al_2 the bonding situation is simpler. Each Al_2 atom is bonded to two oppositely oriented V atoms. Each Al_2–V–Al_2 bonding configuration forms a part of the $\cdots$–Al_2–V–Al_2–V–$\cdots$ chains of bonds that extend over the whole crystal. The chains intersect at each V site and together form a tetrahedral network.

The linear bonding Al_2–V–Al_2 configurations are oriented in the elementary cell of the cubic $Al_{10}V$ structure parallel to face diagonals. For the symmetry analysis it is convenient to rotate the bonding configuration around a vanadium atom in such a way that the trigonal axis of the distorted octahedron coincides with the z-axis. The point group symmetry of the vanadium bonding configuration can be then identified as D_{3d}. The symmetrized orbitals that have to be constructed are oriented from the central V atom to six Al_2 located at vertices of the distorted octahedron. The hybridized orbitals form a reducible representation of the D_{3d} group. Reduction yields four one-dimensional representations (A_{1g}, A_{1u}, A_{2g}, A_{2u}) and two two-dimensional representations (E_g and E_u). Considering that on the V atom there are only s and d orbitals, the assignment of atomic orbitals to irreducible representations with the same transformation properties is the following: A_{1g}: s or d_{z^2}; E_g: (d_{zx}, d_{yz}) or ($d_{x^2-y^2}$, d_{zx}). The symmetrized hybrid orbitals on the V atom can thus be constructed as linear combinations of orbitals with A_{1g} and E_g symmetry. We considered several possible hybridized orbitals and looked for that providing the largest overlap with the hybrid orbitals on the Al_2 atoms. From the side of the aluminium atoms the bonding is clear. It is sp hybridization. On the vanadium side one can consider, e.g., d^3 hybridization consisting of the d_{z^2} orbital with A_{1g} symmetry and two d_{zx}, d_{yz} orbitals with E_g symmetry. We have found that admixing an s orbital with the d_{z^2} orbital provides larger overlap and better describes the bonding situation.

To calculate the COOP for the Al_2–V–Al_2 bonding configuration it was necessary to rotate the symmetrized orbitals in the directions of the actual positions of the atoms in the elementary cell. This was achieved by transformation of the hybrid orbitals using the Wigner $D^l_{m,m'}(\alpha, \beta, \gamma)$ functions, where α, β, and γ are the corresponding Euler angles.

Figure 6(a) shows the COOP for the bonding between V and two Al_2 atoms. One can see that while below the Fermi level the projected DOS is almost entirely bonding, above the Fermi level the bonding is substantially reduced and antibonding states prevail. The COOP, as a difference between bonding and antibonding states, thus changes sign almost exactly at the Fermi level. Moreover, above the Fermi level there is a gap of 0.8 eV where there are no bonding and no antibonding states. This split of bonding and antibonding states demonstrates the covalent character of the Al_2–V–Al_2 bond.

6.2. Bonding between Al atoms in the skeleton of the Friauf polyhedron

From the charge density analysis we found that in the characteristic bonding configuration of Al_3 atoms on the Friauf polyhedron each Al_3 has three Al_3 neighbours. Although the configuration of these three neighbouring atoms around the central atom is neither planar nor forms an equilateral triangle, the dominant contribution to the bonding comes here from the sp^2 hybrid orbitals. It is possible to consider also sp^3 orbitals with orientation of hybrid orbitals in the tetragonal direction, pointing from the three Al_3 neighbours considered and also in the direction towards Al_2. However, in this case the bonding was found to be substantially weaker.

A three-dimensional picture of the bonding in the skeleton of the Friauf polyhedron is seen in figure 2(b). The skeleton has the form of a truncated tetrahedron. The skeleton has 18 edges; each of them represents a covalent Al_3–Al_3 bond. For full saturation of all bonds one needs 36 electrons. These electrons can be provided just by the twelve aluminium atoms that form the skeleton.

Figure 6(b) shows the COOP for the bonding of two Al_3 atoms. Also here one can see that while below the Fermi level the projected DOS is almost entirely bonding, above the Fermi level the bonding is reduced and antibonding states prevail. The COOP, as a difference between bonding and antibonding states, changes sign a little above the Fermi level. Although the character of the COOP demonstrates the covalency of the Al_3 bond, the bond is obviously not fully saturated. This seems to be the consequence of deviation of the actual bonding geometry from the ideal triangular geometry favoured by the sp^2 bonding.

7. Relation to other phases

$Al_{10}V$ is a low-temperature phase stable up to 933 K. We investigated the stability of this phase with respect to the $Al_{21}V_2$ phase differing from $Al_{10}V$ by having occupied centres of the Friauf polyhedra and a hypothetical $Al_{12}V$ phase in the structure of $Al_{12}W$ which exist in the aluminium-rich part of phase diagrams of many Al–TM compounds. $Al_{12}W$ is by composition very close to $Al_{10}V$, but its structure is substantially simpler than that of $Al_{10}V$. It is a bcc packing of Al icosahedra centred on a TM atom. $Al_{10}V$ should also be more stable than a mixture of neighbouring phases, namely pure Al, $Al_{45}V_7$, $Al_{23}V_4$, and Al_3V. $Al_{45}V_7$ and $Al_{23}V_4$ are also quite complex structures. $Al_{45}V_7$ has a monoclinic structure: mC104 in Pearson's notation [12]. It can be considered as an approximant to a decagonal phase. $Al_{23}V_4$ adopts a hexagonal hP54 structure. It can be seen as a packing of overlapping aluminium icosahedra centred on vanadium atoms. On the other hand, the DO_{22} structure of Al_3V is relatively simple. It can be seen as a special decoration of a fcc lattice by Al and V atoms.

The results of the total energy calculations are presented in table 2 and in figure 7. The results essentially agree with the expectations from the experimental phase diagram. The total energy of $Al_{12}V$ is 8.9 meV above the tie-line joining fcc Al and the $Al_{10}V$ phase. The total energy of $Al_{21}V_2$ is 6.5 meV above the tie-line. For $Al_{21}V_2$ we calculate an equilibrium lattice constant of a 14.49 Å, which is only 0.2% larger than that for $Al_{10}V$, demonstrating

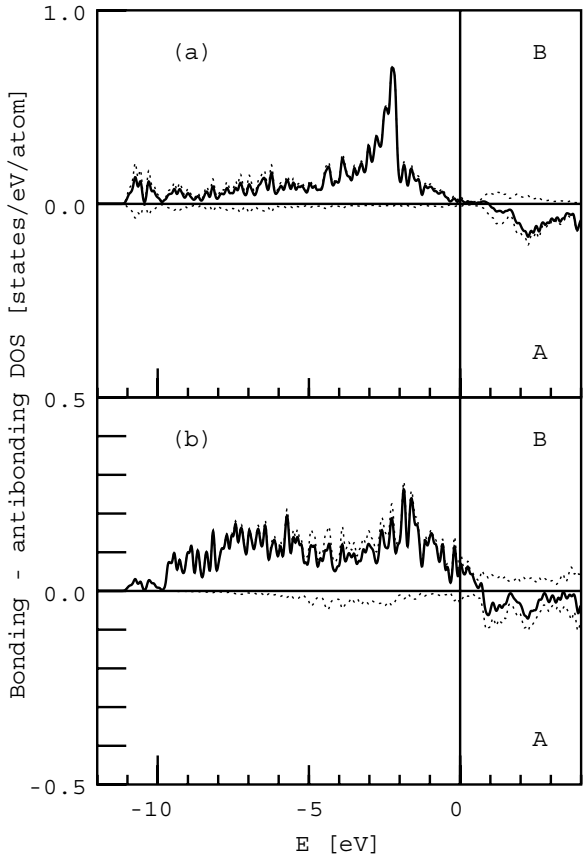

Figure 6. The COOP. The DOS is projected on bonding (B) and antibonding (A) combinations of symmetrized orbitals located on atoms (cf the text). In addition to the bonding density and antibonding density to which, for the sake of clarity, a negative sign is assigned—the two dotted curves—the difference (B − A) between the bonding and antibonding densities is presented (thick curve). (a) The bonding between $V(sd^3)$ and $Al_2(sp)$. (b) The bonding between a pair of $Al_3(sp^2)$ in the skeleton of the Friauf polyhedron.

that the framework of the structure is essentially unchanged by the filling of the empty centre of the Friauf polyhedron by Al. For the volume per atom, this corresponds to a considerable reduction. The remarkable positive excess volume per atom found for $Al_{10}V$ is reduced from 5.8 to 1.7%.

The total energies of $Al_{45}V_7$ and $Al_{23}V_4$ lie precisely on the tie-line joining the $Al_{10}V$ and Al_3V phases. We calculated the electronic structure and also investigated the charge density distribution in these phases. Although their structures are quite different to that of $Al_{10}V$, here again we found chains of covalently bonded aluminium and vanadium atoms. In $Al_{10}V$ the $\cdots$–Al_2–V–Al_2–V–$\cdots$ chains form a tetrahedral network which can be considered as a set of tetrahedrally oriented Kagomé planes; in $Al_{23}V_4$ we have a set of parallel Kagomé planes formed by covalently bonded $\cdots$–Al_2–V–V–Al_2–$\cdots$ chains. The same chains of bonds were found also in $Al_{45}V_7$.

The void inside the Friauf polyhedron may be occupied not only by an Al atom but also by a rare-earth metal. There exists e.g. an isostructural $Al_{20}V_2Eu$ phase [12] where we found the same bonding picture as for $Al_{10}V$. The presence of Eu atoms inside the Friauf polyhedra

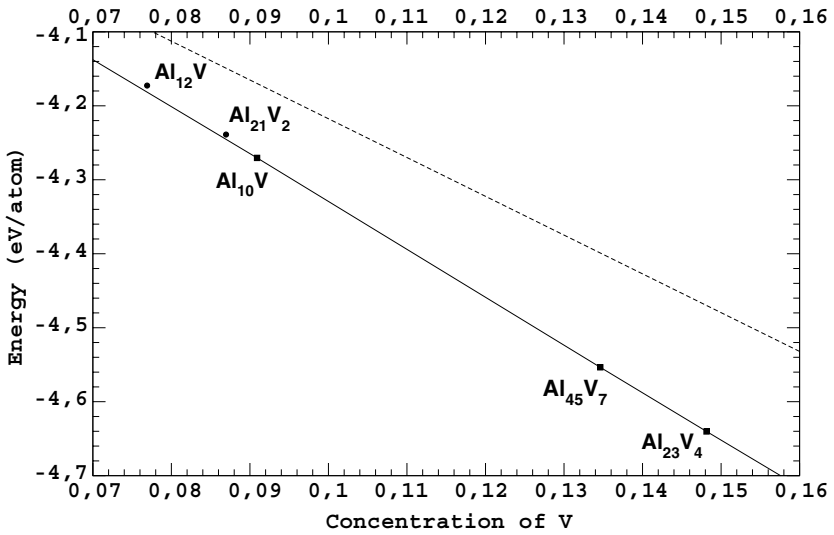

Figure 7. Total energies of $Al_{12}V$, $Al_{21}V_2$, $Al_{10}V$, $Al_{45}V_7$, and $Al_{23}V_4$. The full line is a tie-line joining the total energies of the stable phases Al, $Al_{10}V$, $Al_{45}V_7$, $Al_{23}V_4$, and Al_3V. The total energy of $Al_{12}V$ is 8.9 meV above the tie-line joining fcc Al and the $Al_{10}V$ phase. The total energy of $Al_{21}V_2$ is 6.5 meV above the tie-line. The dashed line joins total energies of fcc Al and bcc V.

Table 2. Total energies $E_{\rm tot}$, heats of formation ΔH, equilibrium volumes per atom V, and excess volumes of formation ΔV for the aluminium-rich vanadium phases. $\Delta E_{\rm tot}$ is a difference of total energies relative to the tie-line joining the total energies of neighbouring stable phases.

Structure	V content (%)	$E_{\rm tot}$ (eV)	$\Delta E_{\rm tot}$ (meV)	ΔH (eV)	V (Å^3)	ΔV (%)
$Al_{12}V$	7.69	−4.1727	8.932	−0.0762	16.73	2.71
$Al_{21}V_2$	8.69	−4.2388	6.466	−0.0897	16.54	1.71
$Al_{10}V$	9.09	−4.2704	—	−0.1001	17.18	5.76
$Al_{45}V_7$	13.46	−4.5534	—	−0.1545	16.18	0.49
$Al_{23}V_4$	14.81	−4.6401	—	−0.1703	16.12	0.41
Al_3V	25.00	−5.2862	—	−0.2824	14.71	−6.35

does not disturb the bonding at the atoms on the surrounding polyhedron, nor that along the Al–V–Al chains. The magnetic moments of Eu atoms are close to the limiting value of 7 $\mu_{\rm B}$ set by Hund's rule.

A considerable variety of isostructural ternary $Al_{20}Cr_2RE$ phases have been reported [12], where the third rare-earth metal constituent is La, Ce, Pr, Nd, Eu, Gd, Ho, Er [12]. Also $Al_{20}Cr_2Y$ and $Al_{20}Cr_2U$ phases were reported [12]. All the above-mentioned ternary phases belong to the $Al_{18}Cr_2Mg_3$ structural class [12]. As was already noted, the $Al_{10}V$ structure can also be considered as a special case of this structural class. In this structure there also exists a tetrahedral network of Al–Cr bonds, with the same packing of Friauf polyhedra but here with their centres occupied by Mg atoms. Other Mg atoms are at sites of the Al_1 atoms of the $Al_{10}V$ structure. We have calculated the charge density distribution of $Al_{18}Cr_2Mg_3$ and found the same picture of bonding in this structure also—the tetrahedral network of Al–Cr bonds, and strongly bonded skeletons of Friauf polyhedra consisting of 12 aluminium atoms. Four Mg atoms are weakly bonded to the skeleton and together form the Friauf polyhedron. The centre of the Friauf polyhedron is here occupied by a Mg atom.

8. Discussion and conclusions

On the basis of *ab initio* calculations we analysed the electron density distribution in the elementary cell of the $Al_{10}V$ compound. We found covalent bonding between certain atoms. Each vanadium atom is bonded with three pairs of Al_2 atoms forming a distorted octahedron with D_{3d} symmetry. Each of the three Al_2–V–Al_2 bonding configurations forms a part of the $\cdots$–Al_2–V–Al_2–V–$\cdots$ chains of bonds that extend over the whole crystal. The chains intersect at the V atoms and together form a tetrahedral network. Inside each of the large voids with the form of a truncated Al–V tetrahedron there is a Z_{16} Friauf polyhedron consisting of Al atoms only. Each Friauf polyhedron in the $Al_{10}V$ structure is vertex-connected with four neighbouring Friauf polyhedra via the Al_1 atoms.

The skeleton of the Friauf polyhedron consists of 12 Al_3 atoms. The atoms in the skeleton are strongly bonded. The Al_3–Al_3 bonds have covalent character dominated by sp^2 hybridization. This configuration of 12 atoms with the form of a truncated tetrahedron seems to be at low temperatures more stable than the configuration of an icosahedron. The centre of the Friauf polyhedron may be empty or occupied by an Al atom. At low temperature the $Al_{10}V$ phase with empty centres is more stable than $Al_{21}V_2$ with occupied centres. However, as the difference in total energies is rather small, the observed degree of occupancy of the void at room temperature [21] of around 50% seems to be reasonable. At temperatures higher than 933 K the configuration of 12 atoms in the form of a truncated tetrahedron probably collapses to an icosahedral configuration.

The void inside the Friauf polyhedron may be occupied not only by an Al atom, but also by a rare-earth metal. There exists, e.g., an isostructural $Al_{20}V_2Eu$ phase where we found the same bonding picture as for the $Al_{10}V$. The presence of Eu atoms inside the Friauf polyhedra does not disturb the surrounding bonds.

$Al_{20}V_2Eu$ belongs to the $Al_{18}Cr_2Mg_3$ structural class. This structural class includes also many other interesting aluminium-rich phases. Although $Al_{10}Cr$ isostructural with $Al_{10}V$ has not been reported, there exist many $Al_{20}Cr_2M$ phases, where M may be Y, La, Ce, Pr, Nd, Eu, Gd, Ho, Er, or U. It seems that almost any big atom with two or three valence electrons may occupy the void in the Friauf polyhedron.

All the above-mentioned ternary phases are isostructural with the $Al_{18}Cr_2Mg_3$ structural class. We have found in this structure the same bonding features—a tetrahedral network of Al–Cr bonds, and strongly bonded skeletons of Friauf polyhedra consisting of 12 aluminium atoms. Four Mg atoms are weakly bonded to the skeleton and together form the Friauf polyhedron. The centre of the Friauf is here occupied by a Mg atom.

We consider the observed chains of covalent bonds –Al_2–V–Al_2–V– and –Al_2–Cr–Al_2–Cr– that extend over the whole crystal a particularly significant feature of the bonding in these alloys. As similar chains of covalent bonds were found also in other aluminium-rich Al–V and Al–Cr alloys, this could suggest a possible explanation for the anomalously high mechanical strength of aluminium-rich Al–V–Fe and Al–Cr–Co–Ce alloys [2] with nanocrystalline or quasicrystalline structures. However, this is so far only a conjecture, which deserves more detailed investigation.

The Friauf polyhedra in the $Al_{10}V$ structure form a diamond lattice. It is remarkable that the $Al_{10}V$ structure may be considered as a 'super-Laves phase' (C15 Cu_2Mg-type) where the Friauf polyhedra play the role of big Mg atoms and where the polytetrahedral Kagomé network of Cu atoms is replaced by a V–Al_2 network. This observation may have an interesting implication. It is well known that the C15 Laves phase is related to quasicrystals. The primitive cell of Cu_2Mg has the form of a rhombohedron that has the same decoration as the golden prolate rhombohedron in the (Al, Zn)Mg quasicrystal. This suggests that $Al_{10}V$ structure

may be similarly related to an aluminium-rich vanadium quasicrystalline phase that has been observed but not yet thoroughly investigated [1, 2].

Acknowledgments

This work was supported by the Austrian Ministry for Science through the Centre for Computational Materials Science. MK also acknowledges support from the Grant Agency for Science in Slovakia (Grant No 2/2038/22).

References

[1] Inoue A and Kimura H 2000 *Mater. Sci. Eng.* A **286** 1
[2] Inoue A, Kimura H, Sasamori K and Masumoto T 1996 *Mater. Trans. JIM* **37** 1287
[3] Stadnik Z M (ed) 1999 *Physical Properties of Quasicrystals* (*Springer Series in Solid-State Sciences vol 126*) (Berlin: Springer)
[4] Krajčí M and Hafner J 2002 *J. Phys.: Condens. Matter* **14** 5755
[5] Krajčí M and Hafner J 2002 *J. Phys.: Condens. Matter* **14** 7201
[6] Krajčí M and Hafner J 2002 *J. Phys.: Condens. Matter* **14** 1865
[7] Dunlop J B, Grüner G and Caplin A D 1974 *J. Phys. F: Met. Phys.* **4** 2203
[8] Lue C-S, Chepin S, Chepin J and Ross J H Jr 1998 *Phys. Rev.* B **57** 7010
[9] Caplin A D, Grüner G and Dunlop J B 1973 *Phys. Rev. Lett.* **30** 1138
[10] Frank F C and Kasper J S 1958 *Acta Crystallogr.* **11** 184
[11] Brown P J 1956 *Acta Crystallogr.* **10** 133
[12] Villars P and Calvet L D 1991 *Pearson's Handbook of Crystallographic Data for Intermetallic Phases* vol 1, 2nd edn (Materials Park, OH: American Society for Metals)
[13] Samson S 1958 *Acta Crystallogr.* **11** 851
[14] Hoffmann R 1988 *Solids and Surfaces: a Chemist's View of Bonding in Extended Structures* (New York: VCH)
[15] Kresse G and Furthmüller J 1996 *Comput. Mater. Sci.* **6** 15
Kresse G and Furthmüller J 1999 *Phys. Rev.* B **54** 11160
[16] Kresse G and Joubert D 1999 *Phys. Rev.* B **59** 1758
[17] Andersen O K 1975 *Phys. Rev.* B **12** 3060
Skriver H L 1984 *The LMTO Method* (Berlin: Springer)
[18] Andersen O K, Jepsen O and Götzel D 1985 *Highlights of Condensed Matter Theory* ed F Fumi and M P Tosi (New York: North-Holland)
[19] Andersen O K, Jepsen D and Šob M 1987 *Electronic Band Structure and its Applications* ed M Youssouff (Berlin: Springer)
[20] Trambly de Laissardière G, Nguyen Manh D, Magaud L, Julien J P, Cyrot-Lackmann F and Mayou D 1995 *Phys. Rev.* B **52** 7920
[21] Ray A E and Smith J F 1957 *Acta Crystallogr.* **10** 604